IEICE TRANS. ELECTRON., VOL.E85-C, NO.1 JANUARY 2002

PAPER *Special Issue on Ultrafast Optical Signal Processing and Its Application*

Design of $LiNbO_3$ Optical Modulator with an Asymmetric Resonant Structure

Tetsuya KAWANISHI[†a)], Satoshi OIKAWA[††], Kaoru HIGUMA[††], Masahide SASAKI[†], *and* Masayuki IZUTSU[†], *Regular Members*

SUMMARY $LiNbO_3$ optical modulators for bancl-operation with a resonant modulating electrode are investigated in this paper. We propose an asymmetric resonant structure consisting of' two arms of modulating electrodes, where one arm is open-ended and the other arm is short-enbed. The voltage standingwave was enhanced by the resonance of the electrodes, so that effective optical modulation was achieved, while the length of the modulating electrode was much shorter than the conventional travelingwave-type electrodes. Tlre optical response at, 6.2GHz of a resonant. modulator designed by maximizing the normalized inducecl phase was 4.94 of the response at dc with a non-resonant modulator.
key words: *optical modulator, resonance, asymmetric structure, waveguide, impedance matching*

1 . Introduction

High-Speed optical modulators are key devices used in wide-band communication systems. In conventional modulators, traveling-wave electrodes are used to achieve broad-band optical response up to the millimeter wave region [1]-[4]. The velocity of an electric guided wave on a traveling-wave electrode matches that of a lightwave propagating in an optical waveguide. The electric field induced by the guided wave can interact with the lightwave, while the guided wave propagates on the electrode. Thus, the interaction can be enhanced by using a long traveling-wave electrode in the broad-band region (ex. dc-40 GHz) . On the other hand, band-operation optical modulators are required in radio-on-fiber systems [5],[6]. By using resonant structures, we can obtain effective optical modulation in a, particular band [7]-[9].

The voltage on the modulating electrode can be enhanced by the resonance of transmission lines, which increases the efficiency of the optical modulation even with a Short electrode. If the feeding point of the modulating electrode is close to the node of the standing-wave voltage profile, the peak voltage on the electrode is muc.h higher than the voltage at the feeding point. However, the impedance at the feeding point is low, so that te voltage at the feeding point is also low. Thus, the peak voltage is low in relation to the input voltage. To enhance the peak voltage, it is necessary to increase the impedance at the feeding point, while keeping thc feeding point close to the node of the standing wave. Sasaki and Izutsu (1997) proposed an optical modulator for band-operation. It consisted of two resonant electrodes with a patch capacitance at the feeding point [10]. The two electrodes were the same length; they were slightly longer than one-quarter or three-quarters of the wavelength propagating on thc electrode. the impedance of the electrodes is inductive and very small. The patch capacitance was designed to match the impedance at the feeding point, between the feeding line and the combined impedance of the electrodes and the capacitance. However, the modulator described in the previous work is difiicult to make because its patch capacitance consisted of a complicated three-dimensional structure. In the work described in this paper, we investigated a resonant-type Mach-Zehnder optical modulator consisting of planar structures, designed to overcome the problems of making such a device and to increase the efficiency of the optical modulation.

2. Asymmetric Resonant Structure

As shown in Fig1, the modulating electrode has two arms that are asymmetric coplanar waveguides (ACPWs). the ground plane, modulating electrode, and feeding line consist of gold whose thickness is t_{EL}, where s is the width of the gap between the ground plane and thc rnodulating electrode, and ω is the width of the modulat,ing elec.trode. The feeding line, which is connected at the junctlon of the two arms, is a coplanar waveguide. A buffer layer, whose thickness is t_{BUF}, is there to reduce the loss of the lightwave propagating in the optical waveguides under the metal electrodes. The short arm (Arm I), with length denoted by L_1, is short-ended, while the long arm (arm II), with length denoted by L_2, is open-ended. the two arms differ in length and termination, so that we termed this configuration the asymmetric resonant structure. The equivalent circuit is shown in Fig. 2, where the impedance of Arm I (Z_1) and that of arm II (Z_2) are expressed by

Manuscript received May 23, 2001.
Manuscript revised July 26, 2001.
[†]The authors are with Communications Research Laboratory, Koganei-shi, 184-8795 Japan.
[††]The authors are with New Technology Research Laboratories, Sumitomo Osaka Cement, Funabashi-shi, 274-8601 Japan.
a) E-mail: kawanish@crl.go.jp

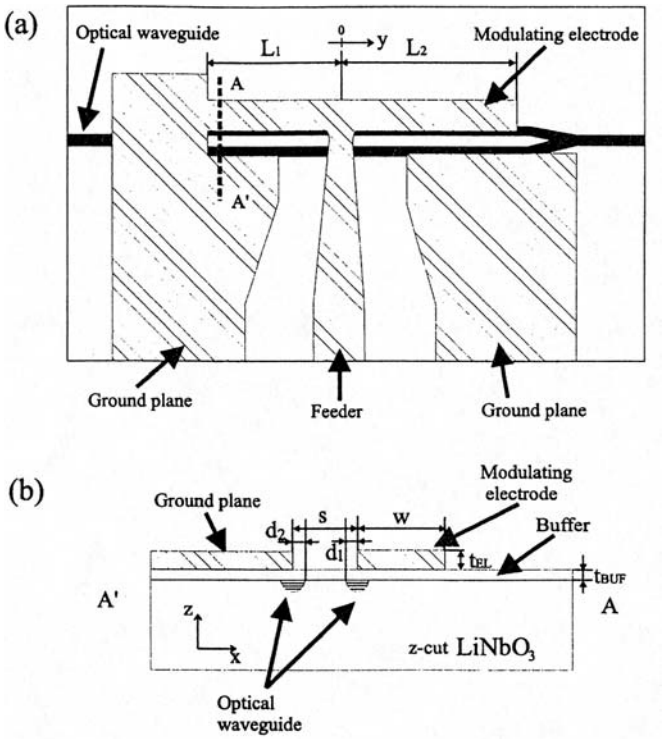

Fig. 1 Structure of an optical modulator with an asymmetric resonant structure. (a) top view, (b) cross-section.

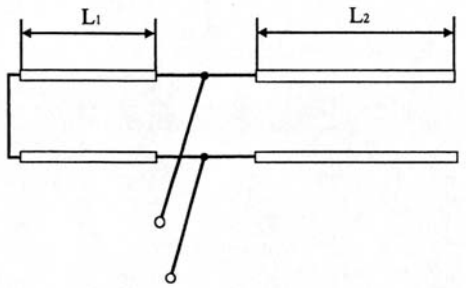

Fig.2 Equivalent circuit for the asymmetric resonant electrode.

$$Z_1 = Z_0 \tanh \gamma L_1 \tag{1}$$
$$Z_2 = Z_0 \coth \gamma L_2. \tag{2}$$

Z_0 is the characteristic impedance of ACPW. γ(= α+ jβ) denotes the propagation coefficient. The total impedance of the asymmetric resonant structure is given by

$$Z_L = Z_0 \frac{\tanh \gamma L_1 \coth \gamma L_2}{\tanh \gamma L_1 + \coth \gamma L_2}. \tag{3}$$

The voltage on the modulating electrode is given by

$$V(y,t) = \mathrm{Re}\left[TG(y)V_{in}\mathrm{e}^{\mathrm{j}2\pi f(t-t_0)}\right], \tag{4}$$

where $V_{in}\mathrm{e}^{\mathrm{j}2\pi f(t-t_0)}$ is the input voltage whose frequency is f. For simplicity, we assume V_{in} = 1. The voltage transmittance at the junction is defined by

$$T \equiv \frac{2Z_L}{Z_L + Z_f}, \tag{5}$$

where Z_f is the characteristic impedance of the feeding line. $|T|$ is an increasing function of $|Z_L|$, and the range is from 0 ($|Z_L| = 0$) to 2 ($|Z_L| = \infty$).

$G(y)$ expresses the distribution of the standing voltage wave on the electrode and is defined by

$$G(y) \equiv \begin{cases} \dfrac{\cosh \gamma(L_2 - y)}{\cosh \gamma L_2} & (y > 0) \\ \dfrac{\sinh \gamma(L_1 + y)}{\sinh \gamma L_1} & (y < 0) \end{cases}. \tag{6}$$

The induced phase at each optical waveguide is the sum of the Pockels effect with respect to the coordinate system moving along with the lightwave propagating in the optical waveguide. Thus, the difference of the induced phases of the two optical waveguides of the Mach-Zehnder structure can be expressed by

$$\phi = \frac{\pi}{\lambda_0} n_0^3 r_{33} \frac{\Gamma}{s} L\Phi \tag{7}$$

$$\Phi \equiv \frac{1}{L}\int_{-L_1}^{L_2} V\left(y, \frac{y}{c}n_0 + t\right) \mathrm{d}y, \tag{8}$$

where c is the speed of light. λ_0 and n_0 are the wavelength and refractive index of the lightwave, respectively. $L \equiv L_1 + L_2$ is the total length of the modulating electrodes. Γ is the overlap integral between the field of the lightwave and the field induced by the electrode. The Pockels effect between the z-direction component of the electric field induced by the modulating electrode and lightwave whose electric fleld is polarized in the z-direction is considered, because the electrooptic coefficient of the effect mentioned above (r_{33}) is the largest one. The factor of $\frac{y}{c}n_0 + t$ means the phase difference due to the propagation delay of the lightwave.

The integral of the voltage on the electrode defined by Eq. (8), Φ, is termed normalized induced phase, and shows the effect of the resonant structure. The normalized induced phase for an optical modulator with a resonant structure can be larger than unity, while the normalized induced phase for a lossless perfectly velocity-matched traveling wave modulator equals unity. The half-wave voltage of the modulator V_π is given by π/ϕ. Similarly, $V_\pi L$, defined by $\pi L/\phi$ ($\propto \Phi^{-1}$), is the voltage-1ength product which shows the degree of the modulation efficiency and the scale of the modulator. To obtain compact and effective optical modulators for band-operation, we designed them to have large normalized induced phases, as shown in following sections.

3. Design by Maximizing the Normalized Induced Phase

We consider a ACPW with the following: t_{BUF} =

Table1 Dependence of the propagating constant and the characteristic impedance of th modulating electrode on the width of the electrode.

w[μm]	α[1/m]	β[rad/m]	Z0[Ω]
5	25.92	735.2	70.10
10	21.16	808.0	55.68
20	16.54	851.9	45.22
50	11.24	891.8	34.71

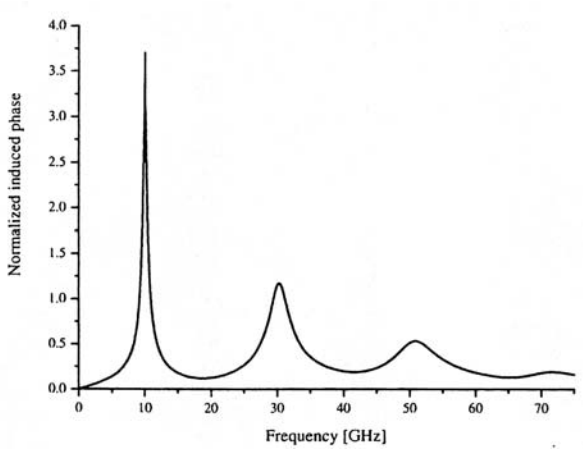

Fig. 3 Optical response of a designed modulator, where L_1 = 0.03 λ and L_2) = 0.22 λ.

0.55 μm, s = 27 μm, and t_{EL} = 2 μm. Dependence of γ and Z_0 on ω at 10GHz Was calculated by using an electro-magnetic field calculator with the finite element method (HP-HFSS5.4), as shown in Table 1. To reduce the loss α, ω was set to be 50 μm. Thus, the wavelength of a 10GHz Voltage wave on the ACPW ($\lambda = 2\pi/\beta$) was 7.03mm. The following parameters were used for numerical calculations: ϵ_{SiO_2} = 4.0, $\epsilon_{LiNbO_3[xy]}$ = 43.0, $\epsilon_{LiNbO_3[z]}$ = 28.0 and σ_{Au} = 4.3 x 10^7 $(\Omega m)^{-1}$. $\epsilon_{LiNbO_3[xy]}$ and $\epsilon_{LiNbO_3[z]}$ denote permittivities of $LiNbO_3$ in the xy-plane and the z-direction, respectively. ϵ_{SiO_2} and σ_{Au} are permittivity of the buffer layer (SiO_2) and conductivity of the electrodes (*Au*), respectively.

By using Eqs. (7) and (8), we obtained a combination of L_1 and L_2, which gave a maximum of Φ. When L_1 = 0.03λ and L_2 = 0.22λ, Φ had a maximum of 3.7 at 10 GHz. Figure 3 shows the normalized induced phase as a function of the frequency f. In addition to a peak at 10GHz, there are peaks due to high-order resonance at 30 and 50 GHz. In Fig. 4, the voltage reflectivity at the junction and the total impedance of these two modulating electrodes were shown as functions of f. The denominator of Eq. (3) goes to a minimum at resonance, which corresponds to parallel resonance of the two arms, so that the impedance has peaks at the resonant frequencies (10, 30, 50, and 70 GHz). As shown in Fig. 4, the reflectivity has dips, where the impedance has peaks. The peaks of the optical response were caused by enhancement of T. Actually, the impedance Z_L is not edual to Z_f at the first-order resonance (10GHz), as shown in Fig. 5. The impedance matching performed at the feeding point is not necessary to obtain a large optica1 response, because the Pockels effect is caused by the electric field induced by the electrodes regardless of the power inputted from the feeding line.

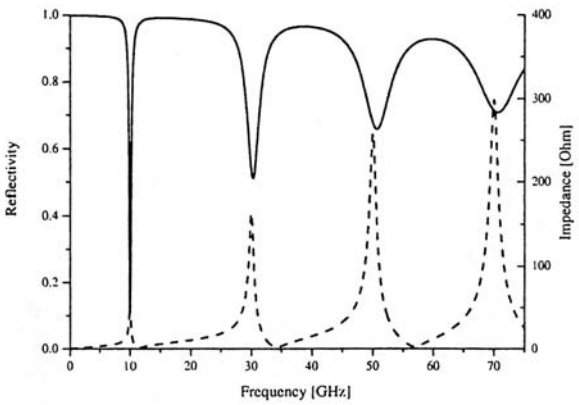

Fig. 4 Electric response of a designed modulator. Solid line and dashed line denote voltage reflectivity at the junction and impedance of the asymmetric resonant structure, respectively, where L_1 = 0.03 λ and L_2 = O.22λ.

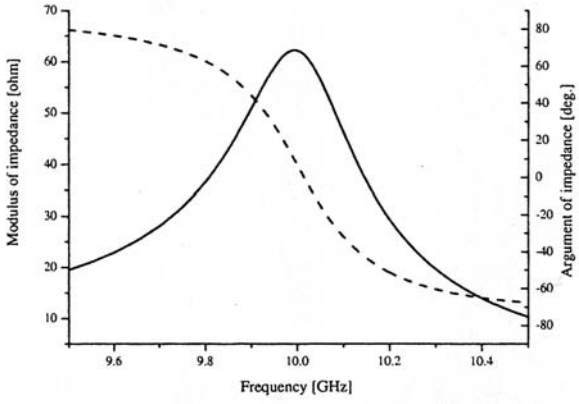

Fig. 5 Impedance of the modulator near the peak at 10 GHz. Solid line and dashed line denote modulus and argument of the impedance.

If both arms were terminated by the same impedance (e.g. open or short), the polarity of the standing-wave voltage profille would change on the electrodes and the length L_1 or L_2 should be longer to obtain the resonance. In an asymmetric resonant structure, however, both L_1 and L_2 are smaller than a quarter of the wavelength λ. As shown in Fig.6, the polarity does not change, which is why an asymmetric structure can reduce the half-wave voltage and the electrode length. At the end of Arm II, the voltage amplitude is approximately six times as large as the input voltage. The length of Arm II is slightly shorter than λ/4, so that Arm II is nearly in resonance and that the

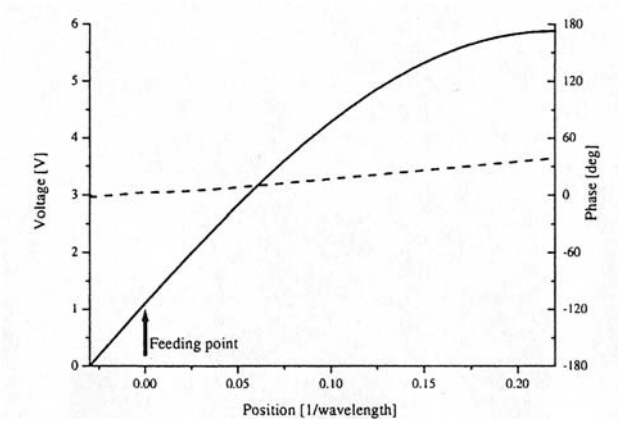

Fig.6 Voltage wave distribution on modulating electrodes, with respect to the corrdinate system moving along with the lightwave propagating in the optical waveguide $V(y, \frac{y}{c} n_0 + t)$. Solid line and dashed line denote the amplitude and the phase of the voltage wave, respectively.

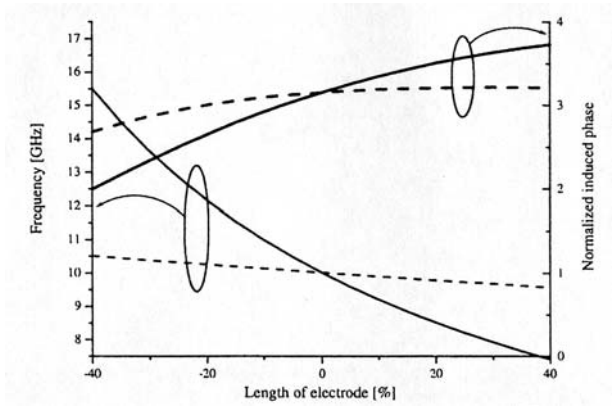

Fig. 7 Dependence of the optlcal response on the lengths of the modulating electrodes. Solid lines denote the resonant frequency of the optical response and the induced phase at the resonance as functions of variation of L_1. Dashed lines show the resonant frequency and the induced phase as functions of variation of L_2.

impedance of Arm II is small. But, thc total impedance Z_L is large owing to Arm I which has two functions: as a stub to enhance the impedance and as a modulating electrocle. Arms I ancl II are in parallel resonance, where Arm I is capacitive and Arm II is inductive. In addition, the resonance can occur even when the length L_1 or L_2 are slightly varied, as shown in Fig. 7.

4. Design by Maximizing the Peak Voltage

If we neglect the loss of the ACPW, the impedance Z_L can be, approximately, expressed by

$$Z_L = \frac{jZ_0 \sin \beta L_1 \cos \beta L_2}{\cos \beta (L_1 + L_2)}. \tag{9}$$

The impedances of Arms I and II at the feeding point can be also expressecl by $Z_1 = jZ_0 \tan \beta L_1$ and $Z_2 = -jZ_0 \cot \beta L_2$. Because L_1 and L_2 are shorter than a quarter of the wavelength, the impedance of the long

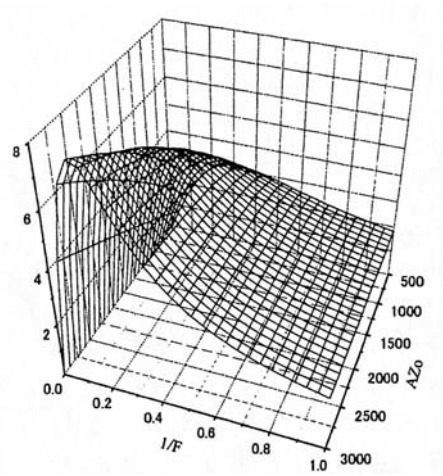

Fig. 8 The ratio of the voltage at the end of Arm II to that of input voltage wave.

arm is capacitive, and that of the short arm is inductive. When $L_1 + L_2 = \lambda/4$, these two arms are in resonance and the denominator of Eq. (9) goes to zero. To obtain the impedance Z_L at the resonance, the denominator should be estimated with taking account of the loss α. We introduce the resonant factor defined by $A \equiv j/\cosh(\gamma\lambda/4)$, so that Z_L can be expressed by $AZ_0 \sin^2 \beta L_1$. In addition, the imaginary part of Z_L is zero at the resonance frequency as shown in Fig. 5 , so that A has a real value. The voltage transmision coefficient at the feeding point can be expressed by

$$T \equiv \frac{2AZ_0 \sin^2 \beta L_1}{AZ_0 \sin^2 \beta L_1 + Z_f}, \tag{10}$$

where Z_f is the characteristic impedance of the feeding line. The profile of the standing voltage wave on the electrode has a peak at the open-end of Arm II. The ratio of the voltage at the feeding point to the voltage at the end of Arm II is given by $F \equiv (\sin \beta L_1)^{-1}$. Thus, an asymmetric resonant structure can be roughly optimized by maximizing the peak voltage, that is, $T \times F$.

The ratio of the voltage at the end of Arm II to the input voltage wave is shown in Fig. 8 as a function of AZ_0 and F. While F is determined by the ratio of L_1 to L_2, AZ_0 depends on the cross-section of the modulating electrode, and can vary with fluctuations in the fabrication process and deformation of the electro-magnetic field at the feeding junction. As shown in Fig. 8, when $1/F$ was nearly equal to 0.2, $T \times F$ was high and did not depend so much on AZ_0, assuming Z_f is 50Ω. Based on numerical calculations using the calculator HP-HFSS5.4 under various conditions, we can assume that $500 < AZ_0 < 3000$. Thus, when $L_1 = 0.03\ \lambda$ and $L_2 = 0.22\ \lambda$, which corresponds to $1/F = 0.2$, both the voltage and modulation efficiency are enhanced, regardless of fluctuations in AZ_0. The obtained parameters L_1 and L_2 coincide with the results designed by the more rigorous method given in

the previous section. Thus, we may say that the simple design procedure shown in this section is useful for the proposed structure, and that the enhancement of the optical response can occur even if some parameters, such as γ and Z_0, varied by the effect which was not included In the equivalent circuit model, or by the fluctuation of the fabrication process.

.

5. Experimental Results

We measured the optical and electrical response of a fabricated modulator having the following: t_{BUF} = 0.55 μm, ω = 50 μm, s = 27 μm, t_{EL} = 2 μm, L_1 = 0.03 λ = 0.21 mm and L_2 = 0.22λ = 1.55mm. Thus, the total length L was 1.76 mm. The central inductor of the feeding line was 50 μm wide and the characteristic impedance was 50Ω. The Mach-Zehnder interferometer consisted of two optical waveguides formed by the titanium diffusion technique on a z-cut $LiNbO_3$ substrate. The refractive index n_0 was assumed to be 2.2 for λ_0 = 1.55 μm. The effective width and depth of the optical waveguides were 10 μm and 8 μm, respectively. The positions of the waveguides were as follows: d_1 = 2 μm and d_2 = 3 μm. The overlap integra1 Γ, ca1culated by TEM approximation [11], was 0.92, where the thickness of the electrode t_{EL} was neglected. The profile of the mode guided in the optical waveguide was elliptic and the field distribution was assumed to be uniform. The modulator also had an open-ended dc-bias electrode to set the Mach-Zehnder switch function to tlre quadrature point. The normalized induced phase can be measured as the ratio of the optical response of a resonant electrode at a particular frequency to that of a non-resonant electrode at dc, where both electrodes were the same length. Γ obtained by the response measured at dc was 0.82. which was 89% of the calculated one. This discrepancy was due to the effect of the thickness of the electrode or deformation of the lightwave field pattern.

As shown in Fig. 9, the optical response for the 1.55-μm region, obtained from the responses of the resonant and dc-bias electrodes, had a peak of 4.94 at 6.2GHz. The halfwave-voltage was 17.9 V at the peak. The fitting curve was obtained by changing the propagation constant γ from the numerically obtained one. γ was set to be 0.4 α + j1.6 β, where α and β are real and imaginary parts of numerically. obtained propagation constant (see Table l). This result may be due to the difference between the numerically calculated wavenumber and the actual one, and to the deformation of the field at the junction. The measured electric response (reflectivity) is also shown in Fig.9. There are three dips near the resonant peak of the optical response. The dips at 5GHz and 8GHz may htwc been caused by a reflection at a connector or a junction.

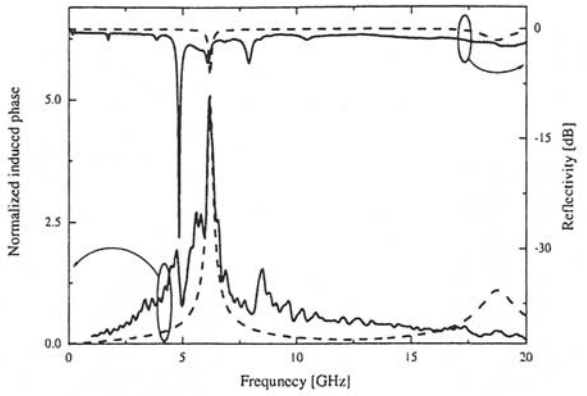

Fig. 9 Responses of the fabricated modulator. Optical responses (normalized induced phase) and electric responses (reflectivity) are shown as functions of the frequency. Solid lines de-note measured responses. Dashed lines denote the fitting curves.

6. Conclusion

An optical modulator with an asymmetric modulating electrode for band-operation was investigated. We proposed two design methods: maximizing the normalized induced phase and maximizing the peak voltage. The latter one is much simpler than the former one, but both methods gave the Same result. The normalized induced phase of the fabricated modulator was 4.94. The half-wave voltage was 17.9 V in the 1.55 μm wavelength range, in spite of the short electrode length of 1.76 mm.

Acknowledgement

We would like to express our appreciation to Dr. Y. Matsuo for his useful discussion.

References

[1] M. Izutsu, H. Haga, and T. Sueta, "0 to 18GHz traveling-wave optical waveguide intensity modulator," IECE Trans., vol.E63, pp.817-818, 1980.
[2] O. Mitomi, K. Noguchi, and H. Miyazawa, "Design of ultra-broad-band $LiNbO_3$ optical modulators with ridge structure," IEEE Trans. Microwave Theory & Tech., vol.43, pp.2203-2207, 1995.
[3] K. Noguchi, O. Mitomi, and H. Miyazawa, "Millimeter-wave Ti:$LiNbO_3$ opitcal modulators," J. Lightwave Technol.,vol.16, pp.615-619, 1998.
[4] K. Noguchi, H. Miyazawa, and O. Mitomi, "40-Gbit/s Ti: $LiNbO_3$ optical modulator with a two-stage electrode," IEICE Trans. Electron., vol.E81-C, pp.1316-1320, 1998.
[5] C. Lim, A. Nirmalathas, D. Novak, and R.Waterhouse, "Optimisation of baseband modulation scheme for millimetre-wave fibre-radio systems," Electron. Lett., vol.36, pp.442-443, 2000.
[6] T. Kuri, K. Kitayama, and Y. Takahashi, "60-GHz-band full-duplex radio-on-fiber system using two-RF-port electroabsorptfon transceiver," IEEE Photon. Technol. Lett., vol.12, pp.419-421, 2000.

[7] Y. Zhou, M. Izutsu, and T. Sueta, "Low-drive-power asymmetric Mach-Zehnder modulator with band-limited operation," J. Lightwave Technol., vol.9, pp.750-753, 1991.
[8] K. Yoshida, A. Nomura, and Y. Kanda, "$LiNbO_3$ optical modulator using a superconducting resonant electrode," IEICE Trans. Electron., vol.E77-C, pp.1181-1184, 1994.
[9] M. Izutsu, T. Mizuochi, and T. Sueta, "Band operation of guided-wave light modulators with filter-type coplanar electrodes," IEICE Trans. Electorn., vol,E78-C, pp.55-60, 1995.
[10] M. Sasaki and M. Izutsu. "High-speed light modulator," FST'97, 1997.
[11] R.E. Collin, Field Theory of Guided Waves, 2nd ed., pp.247-328, IEEE Press, NY, 1991.

Tetsuya Kawanishi received his B.S. and M.S. degrees in electronics from Kyoto University in 1992 and 1994, respectively. He received his Ph.D. in electronics and communication from Kyoto University in 1997. From 1994 to 1995, he had worked at Production Engineering Laboratory of Matsushita Electric Industrical Co., Ltd. From 1997 to 1998, he was a research fellow at Venture Business Laboratory of Kyoto University. Since 1998, he has been with Communications Research laboratory, Ministry of Posts and Telecommunications. His present research activities involve high-speed optical modulation, guided waves in periodic strucutures, and electro-magnetic wave scattering from random surfaces. In 1999, he was awarded URSI Young Scientist Award at URSI-GA 1999.

Satoshi Oikawa received the B.E. and M.E. degrees in electrical engineering from Nihon University, Tokyo, Japan, in 1991 and 1993, respectively. In 1993, he joined Optoelctronics Research Division, New Technology Research Loboratories, Sumitomo Osaka Cement Co., Ltd., Chiba, Japan. He has been engaged in research and development of optical modulators.

Kaoru Higuma received his B.S. degree in physics and M.E. degree in applied optics from Waseda University, Tokyo, Japan, in 1994 and 1996 respectively. In 1996, he joined Sumitomo Osaka Cement Co., where he has been engaged in research and development of optical $LiNbO_3$ modulators.

Masahide Sasaki was born in lwate prefecture, Japan on November 5, 1962. He received the B.S., M.S., and Ph.D. degrees in physics from Tohoku University, Sendai Japan, in 1986, l988 and 1992, respectively. During 1992-1996, he worked on the development of Si-MOSFET with Ayase Laboratory, Nippon Kokan Company, Kanagawa Japan. In 1996, He joined the Communications Research Labolatory. He has been working on the research on millimeterwave-photonic devices, and also on quantum Information technology. Dr. Sasaki is a member of Japanese Society of Physics, and the Institute of Electronics, Information and Communication Engineers of Japan.

Masayuki lzutsu was born in Osaka, Japan, and received the B.Eng., M.Eng., and D.Eng. degrees in electrical engineering from Osaka University, in 1970, 1972, and 1975, respectively. In 1975, he joined the Department of Electrical Engineering, Faculty of Engineering Science, Osaka University, where he worked in the field of guided-wave optoelectronics. From 1983 to 1984, he was a Senior Visiting Research Fellow at the Department of Electronics and Electrical Engineering, University of Glasgow, Scotland. In 1996, he moved in to the Communications Research Laboratory, Ministry of Posts and Telecommunications (from April 1, 2001, Communications Research Laboratory, Independent Administrative Institution), and is now Distinguished Researcher & Acting Leader of Integrated Photonics Group, Basic and Advanced Research Division. Dr. Izutsu received the paper award and the award for significant achievement in 1981 and 1988, respectively, from the Institute of Electronics, Information and Communication Engineers.